Abbas SHIRI, Abbas SHOULAIE

Electrical Engineering Department, Iran University of Science and Technology, Tehran, Iran

Multi-objective optimal design of low-speed linear induction motor using genetic algorithm

Abstract. *In this paper, a simple and applicable procedure is proposed to design single-sided linear induction motor. The designed motor is simulated in MATLAB software in order to investigate the effect of various design variables on the performance of the machine. According to the obtained results, a multi-objective optimization method based on Genetic Algorithm is developed to maximize the efficiency and power factor and to minimize the motor weight, simultaneously. The results show significant enhancement of the objective function. 2D finite element method is used to validate the proposed design.*

Streszczenie. *Zaproponowano metodę projektowania jednostronnego liniowego silnika indukcyjnego z wykorzystaniem programu MATLAB. Do optymalizacji wykorzystano algorytm genetyczny. Poszukiwano maksymalnej skuteczności, małej wagi silnika i małego współczynnika mocy. (**Projektowanie i optymalizacja liniowego silnika indukcyjnego z wykorzystaniem algorytmu genetycznego**)*

Keywords: primary weight, efficiency, optimization, power factor.
Słowa kluczowe: silnik indukcyjny, silnik liniowy, optymalizacja.

Introduction

Primitive Linear motors have been in existence for a long time. However, in recent 3 decades they have taken researchers consideration in industry applications. These kinds of motors are capable of producing linear motion without any need for transmission system and mechanical gears. Among various types of linear motors, linear induction motor (LIM) has gained interest of researchers due to its simple structure. So, great deal of investigations is devoted to these kinds of motors [1-5]. There are different types of LIMs that among them single-sided linear induction motors (SLIMs) are widely used in transportation systems [5, 6]. Proper performance of the SLIM requires optimization of their design, considering different outputs as objective functions.

In order to optimize the LIM, different objective functions have been introduced in literature. In reference [7] the primary weight has been considered as objective function. In other work, the thrust and power to weight ratio are maximized [8]. In [9] and [10] optimum winding design of LIM have been presented. In other researches, optimal design of the LIM for having the maximum efficiency and power factor has been done [11, 12]. In the latter works, the primary current density, the primary width to pole pitch ratio and the secondary aluminum sheet thickness have been selected as design independent variables; While the input frequency and the air-gap length which are important variables in design and affect the performance of the motor, is not considered in the optimization. In [13] imperialist competitive algorithm is used to design SLIM. In this work, the design is not validated by FEM or experiment. In addition, it seems that the flux density in different parts of the motor has not been limited. According to mentioned references and other reports there is not a systematic method for designing SLIMs. In this paper, a computer-aided systematic and applicable design algorithm is proposed for SLIM. In the proposed algorithm, different geometries of the machine are calculated using analytical equations. Then, the low-speed SLIM design is optimized based on the equivalent circuit model and using Genetic algorithm. In order to maximize the efficiency and power factor as well as to minimize the primary weight, all variables which are effective in performance of the SLIM, are considered in optimization. To confirm the validity of the design, finite element method is employed and the results are compared.

Calculation of slot dimensions

The structure of the single-sided linear induction motor as well as its teeth and slot dimensions are shown in Fig.1. In this figure g is the mechanical clearance. Regarding the magnetic permeability of the aluminum, in calculations, the mechanical clearance is replaced with magnetic air gap. The magnetic air gap is defined as:

(1) $$g_m = g + d$$

where d is thickness of the secondary sheet. Considering the concept of current sheet and slotted structure of the primary, the magnetic air-gap will increase to effective air-gap which is given by [14]:

(2) $$g_e = k_c g_m$$

In the above equation, k_c is Carter's coefficient which is given by:

(3) $$k_c = \tau_s /(\tau_s - \gamma g_m)$$

where τ_s is slot pitch and is equal to:

(4) $$\tau_s = \tau /(mq)$$

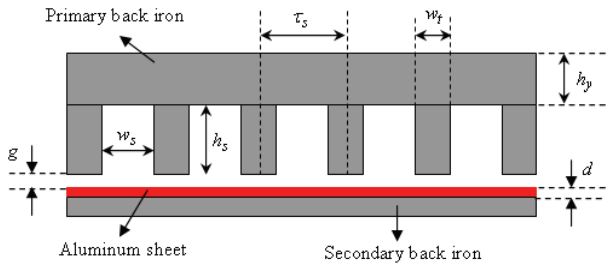

Fig.1. Single-sided linear induction motor

According to [15] γ in equation (3) is given by:

(5) $$\gamma = (w_s / g_m)^2 /[5 + (w_s / g_m)]$$

where w_s is slot width which is calculated by:

(6) $$w_s = \tau_s - w_t$$

In equation (6) w_t is tooth width. The primary slot depth can be simply calculated by the following equation (see Fig. 1):

(7) $$h_s = A_s / w_s$$

where A_s is the cross-sectional area of the primary slot which is given by:

(8) $$A_s = n_c A_w / F_{fill}$$

In the above equation, F_{fill} is fill factor of the slot and n_c is the number of conductors per slot which is equal to:

(9) $$n_c = N / pq$$

where N is the number of turns per phase. Number of turns per coil, n_{coil} can be calculated using n_c. For single layer winding $n_c = n_{coil}$, and for double layer winding $n_c = 2\, n_{coil}$. The cross-sectional area of the conductor of the winding is calculated by:

(10) $$A_w = I_1 / J_1$$

Where I_1 is the primary current and J_1 is primary current density.

Equivalent circuit model of the SLIM

For the design of the SLIM with negligible end effect, the equivalent circuit model is used. The per-phase equivalent circuit model of the SLIM is shown in Fig.2. In this figure R_1 is the per-phase resistance of the primary and is calculated as follows:

(11) $$R_1 = 2(W_s + l_{ec})N / (\sigma_w A_w)$$

In the above equation σ_w is the conductivity of the conductor used in the primary winding. l_{ec} is the end connection length, W_s the primary width, N the number of turns per-phase of the primary winding and A_w is the cross-sectional area of the conductor which is given by equation (10).

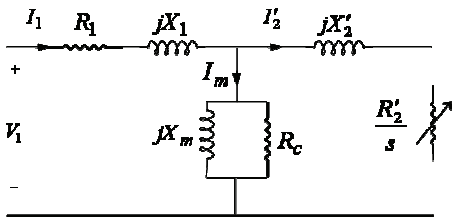

Fig.2. Equivalent circuit of single-sided linear induction motor

The primary leakage reactance is given by [15][16]:

(12) $$X_1 = \left\{ 2\mu_0 \omega_1 [(\lambda_s (1 + \frac{3}{2p}) + \lambda_d) \frac{W_s}{q} + \lambda_e l_{ce}] N^2 \right\} / p$$

where μ_0 is the permeability of the air, p the number of pole pairs, q the number of the slots per pole per phase, ω_1 primary angular frequency and λ_s, λ_e and λ_d are the permeances of slot, end connection and differential, respectively which are given by the following equations[15]:

(13) $$\lambda_s = h_s (1 + 3\beta) / (12 w_s)$$

(14) $$\lambda_e = 0.3(3\beta - 1)$$

(15) $$\lambda_d = 5 g_e / w_s [5 + 4(g_e / w_s)]$$

In the above equations β is the pitch factor of the coil. The per-phase magnetizing reactance of the motor is given by [15]:

(16) $$X_m = 6\mu_0 \omega_1 W_{se} k_w{}^2 N^2 \tau / (\pi^2 p g_e)$$

Where k_w is the winding factor, τ the pole pitch and g_e is the effective air-gap given by equation (2). Also, W_{se} is the equivalent primary width and is calculated by:

(17) $$W_{se} = W_s + g_m$$

The primary referred secondary resistance is defined as[17]:

(18) $$R'_2 = X_m / G$$

Where G is the goodness factor of the motor which is given by [15]:

(19) $$G = 2\mu_0 f_1 \tau^2 \sigma_s d / (\pi\, g_e)$$

in the above equation f_1 is the supply frequency, τ the motor pole pitch and σ_s is the conductivity of the secondary sheet.

With secondary sheet linear induction motors the secondary reactance can be neglected. So, $X'_2 \approx 0$. Also, due to law value of the flux density in the air-gap, core loss is negligible; so, $R_c \approx 0$.

The efficiency of the motor is defined as:

(20) $$\eta = P_o / P_i$$

Where P_o and P_i are output and input power of the motor, respectively. Regarding Fig.2 and replacing proper terms for input and output power, the following equations for efficiency, power factor and thrust are derived:

(21) $$\eta = F_x 2\tau f_1 (1 - s) / [F_x 2\tau f_1 + m I_1{}^2 R_1]$$

(22) $$\cos\varphi = [F_x 2\tau f_1 + m I_1{}^2 R_1] / (m I_1 V_1)$$

(23) $$F_x = m I_1{}^2 R'_2 / (s 2\tau f_1 [(\frac{1}{sG})^2 + 1])$$

where s is the motor slip. The air-gap flux density is given by [15]:

(24) $$B_g = \mu_0 J_m \tau / [\pi g_e \sqrt{1 + (s.G)^2}]$$

in the above equation, J_m is the amplitude of the equivalent current sheet which is calculated as follows [15]:

(25) $$J_m = 3\sqrt{2} k_w N I_1 / (\pi\tau)$$

Using equation (24), the teeth flux density is obtained by:

(26) $$B_t = B_g (\tau_s / w_t)$$

Design procedure

Equation (20) is basically used to initialize the design process in which $P_o = F_x . Vr$; F_x and V_r being the motor thrust and speed, respectively. In this equation, the primary current can be estimated using the desired motor parameters:

(27) $$I_1 = F_{xd} V_r / (m V_1 \eta \cos\varphi)$$

where F_{xd} is the desired thrust should be produced by the designed motor. Now, by having the desired thrust, motor speed, input voltage and proper value for $\eta cos\varphi$, the required input current can be calculated. In this paper, the design procedure is in such way that the motor can finally produce the desired thrust. Thus, to began with, the number of turns per coil (n_{coil}) is set to 1 and increased by 1 until we meet the thrust requirements in the design. In each step the calculated thrust is compared with the desired value. If the error is acceptable the process is stopped. The flow chart of the design is shown in Fig.3. In this flow chart the value of $\eta \cos\phi$ is initially chosen arbitrarily in [0 1] span. Then in the next stage of algorithm its value is compared with the calculated value $[\eta cos\varphi]_{cal}$. If the two values are approximately equal the algorithm is proceeded otherwise the value of $\eta cos\varphi$ replaced by their mean value and the calculation is repeated. Also, in this design in order to prevent the saturation of the iron in teeth, the flux density in teeth is compared with a predefined maximum flux density. If the teeth flux density is higher than its maximum value, the arrangement of the turns in slot is changed.

Table 1 shows the specification of the designed motor. In this design the obtained value of the number of turns per coil, n_{coil} is 87 (single layer winding is used). With this number of turns, the thrust of the motor is approximately equal to its desired value. In addition, the efficiency and the power factor are obtained 46.15% and 0.1921, respectively; and the primary weight is 7.14 kg.

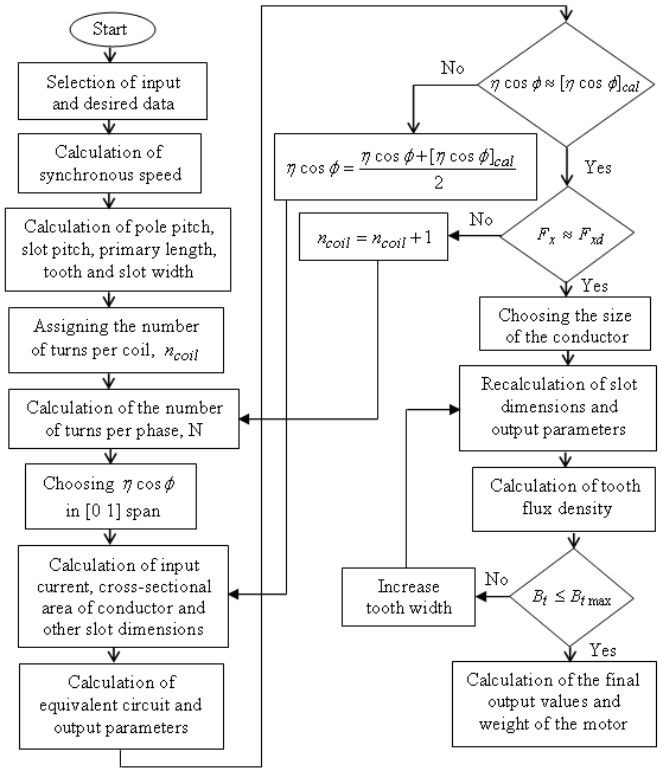

Fig.3. flow chart for the SLIM design

Table 1: The specification of the designed motor

Phase voltage, v	220
Supply frequency, Hz	50
Number of pole pairs,(p)	2
Rated slip	0.3
Number of slots/pole/phase(q)	1
Primary width, mm	150
Thickness of the secondary sheet, mm	3
Primary current density, A/mm^2	5
Desired thrust, N	128
Rated speed, m/s	2.5
Mechanical clearance, mm	1

Simulation results and discussion

In this section, to investigate the effect of design variables such as the secondary sheet thickness, the mechanical clearance, the supply frequency, the primary width, etc. on the SLIM performance, the designed motor is simulated using MATLAB software. The reaction of the motor to independent design variables is important for optimization problem. In these simulations, the motor is designed to have $(128\pm4)N$ output thrust with motor speed of $V_r=2.5m/s$. The input voltage is $V_1=220V$.

In Fig.4, the effect of the primary current density on the motor outputs such as output thrust, primary weight, efficiency, and power factor are illustrated. In this figure, other independent variables are kept constant. Increasing the primary current density with constant output thrust decreases the primary wire cross-section and increases the primary resistance of the motor. So, it causes the primary weight and efficiency to decrease. It also increases the power factor. The output thrust is about the desired value of 128N. As a result, to select a proper value for the primary current density, there should be a compromise between different outputs such as weight, efficiency, and power factor. It is seen that there are some jumps on the curves, especially on output thrust, in the figure. These jumps are because of changing the number of turns per coil in design process to produce the desired thrust. Fig.5 show that increasing the primary width with constant motor length increases the primary weight and power factor, at the same time it decreases the efficiency, although the changes in efficiency are small. By increasing the aluminum thickness, the primary weight of the motor decreases and reaches a minimum value and then increases; while, the power factor and the efficiency increase until they reach a maximum value and then decrease (see Fig.6).

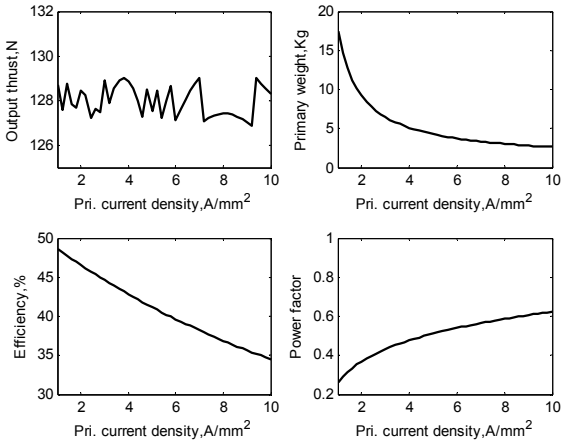

Fig.4. The SLIM outputs versus the primary current density

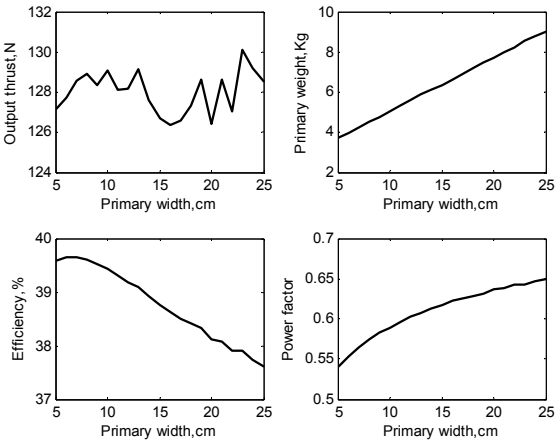

Fig.5. The SLIM outputs versus the primary width

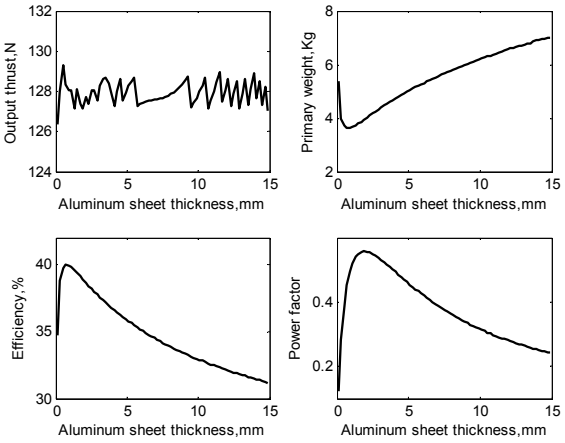

Fig.6. The SLIM outputs versus the aluminum thickness

The variation of the outputs versus the mechanical clearance is shown in Fig.7. It is seen that increasing the mechanical clearance increases the primary weight to produce desired output thrust of about 128N. The efficiency and power factor decrease as the mechanical clearance is increased. As a result, in design process, the air-gap should

be chosen as short as possible to maximize efficiency and power factor, at the same time to minimize the SLIM weight. Fig.8 illustrates the variation of the motor outputs versus number of pole pairs. Increasing the number of poles increases the motor length in constant frequency, synchronous speed, and primary width which leads to the increment of the primary weight. On the other hand, the efficiency reduces by increasing the pole number. In addition, increasing the number of poles increases the power factor. As seen in Fig.9, increasing the number of slots/pole/phase slightly decreases the primary weight. However, it increases the efficiency and the power factor; although, the increment of the efficiency is quite small. Increasing the ratio of slot width to slot pitch decreases the primary weight and increases the power factor, while having negligible effect on efficiency (Fig.10). Fig.11 shows the simulation results of the motor by changing supply frequency. As it is seen in the figure, increasing the frequency decreases the primary weight; at the same time it increases the efficiency. Also, the power factor increases until frequency of about 17Hz and then decreases. Finally, in Fig.12, the effect of increasing motor slip as a design variable on the outputs is shown. As seen in this figure, increasing the slip decreases the SLIM weight; although after the slip of 0.42, the weight increases. Also, by increasing the slip, the efficiency increases until it reaches a maximum value and then decrease; while the power factor increases by increasing the motor slip. According to the above explanations and considering the application of the motor and its limitations, one can develop the design in a way that the motor can produce optimum outputs. In the next section, using genetic algorithm, the design is optimized considering all effective variables of the motor.

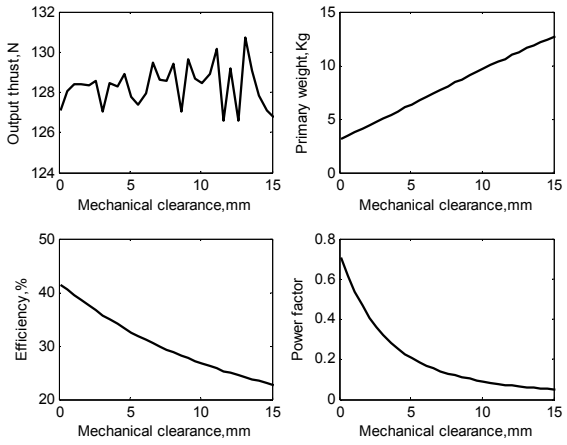

Fig.7. The SLIM outputs versus the mechanical clearance

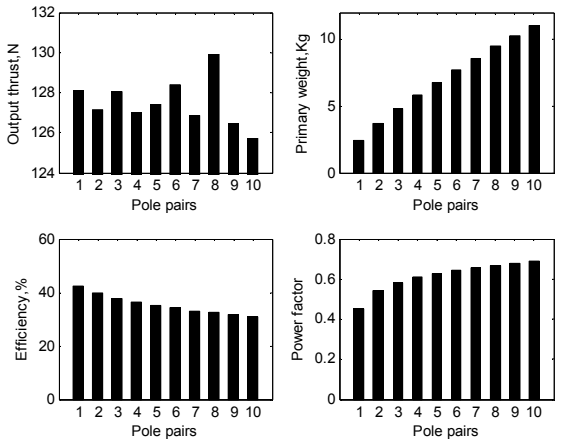

Fig.8. The SLIM outputs versus the number of pole pairs

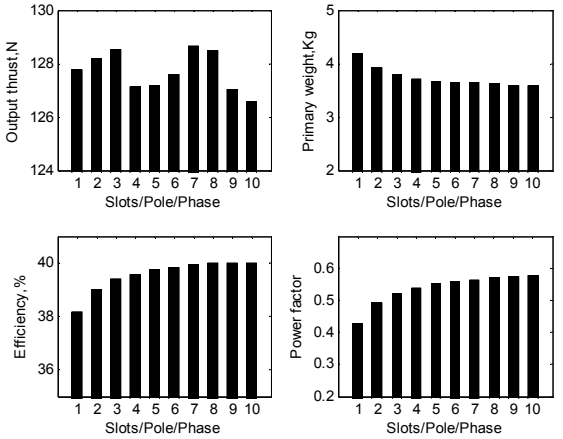

Fig.9. The SLIM outputs versus the number of slots/pole/phase

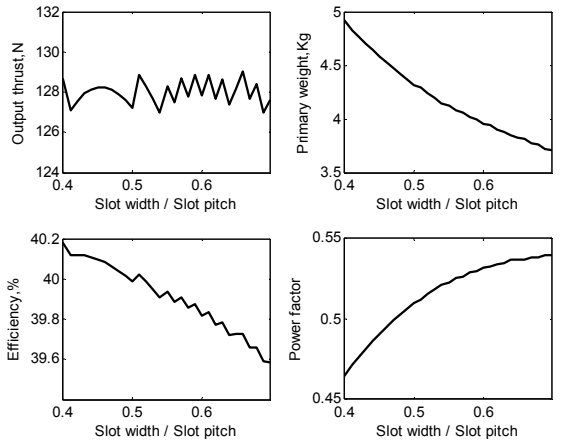

Fig.10. The SLIM outputs versus the slot width/slot pitch

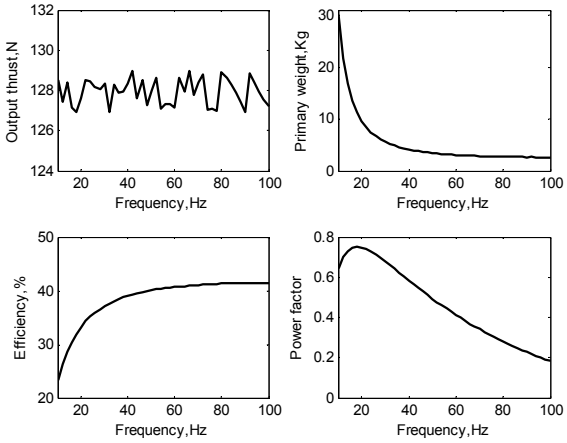

Fig.11. The SLIM outputs versus the supply frequency

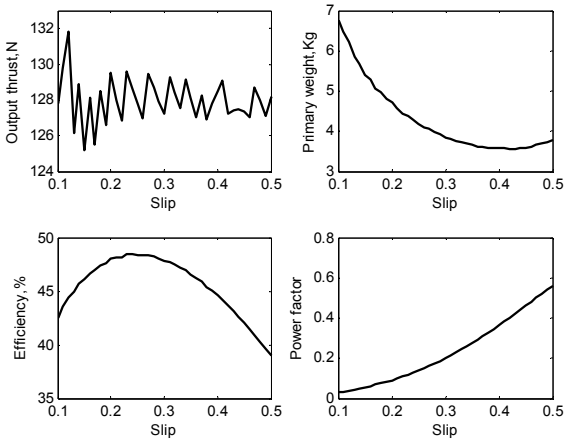

Fig.12.The SLIM outputs versus the slip as a design variable

Genetic algorithm based design optimization

In this paper, nine effective design variables and their ranges of variations is considered for optimization goal. From these ranges, the computer program investigates various potential solutions. For each solution, constraints are evaluated. If all these constraints are satisfied, the value of the objective function is calculated and the solution is considered as an acceptable design. On the other hand, the potential solutions that do not meet the constraints are ignored as non-acceptable designs. Finally, among the acceptable solutions, the final design with the optimum value of the objective function is selected. Considering the results of investigations performed in previous section, in this paper, nine design variables are chosen as follows: primary current density (J_1), the primary width (W_s), the secondary sheet thickness (d), motor slip (s), the mechanical clearance (g), number of pole pairs (p), number of slots per pole per-phase (q), slot width to slot pitch ratio (w_s/τ_S),and the primary input frequency (f_1). In addition, the maximum tooth flux density and the ratio of primary width to pole pitch are applied as optimization constraints:

(28) $$B_{t\max} \le 1.6$$

(29) $$0.5 \le W_s / \tau \le 4$$

Other parameter constraints applied to the design are listed in Table 2.

To optimize the motor, different outputs can be considered as objective function. In this paper regarding the importance of the efficiency, power factor, and the primary weight of the SLIM, the objective function is considered as:

(30) $$f(x) = [\eta(x)^{K_1} \times P.F.(x)^{K_2}]/[\mathrm{Pr}imary\ weight(x)]^{K_3}$$

where x is the optimization variables vector and K_i (i=1...3) can be chosen as 0 or 1. The rated specifications of the motor are the same as those used in previous section. In this paper, genetic algorithm is employed for optimization. The genetic algorithm is a method that searches among different variable values and finds a set of parameters to optimize the objective function [18]. To do this, first initial population is selected randomly. In the next stage, two members as parents are selected among population to reproduce offspring. After recombination of the parents and reproduction of offspring, mutation is done on one of the chromosomes (variables) of offspring to produce new offspring. Two offsprings are compared with each other and one of them is selected as final offspring based on their fitness level. There are many techniques to compare the final offspring with population [18]. In this paper, the final offspring is compared with the least-fit individual in population. If the offspring is better than the least-fit individual, the latter is replaced by the former; otherwise the offspring is eliminated. Flowchart for the genetic algorithm is illustrated in Fig.13. The optimization is done for different objective functions using equation (30). In the first step, K_1=1,K_2=K_3=0. It means that only the efficiency is optimized. In the next step, K_2=1, K_1=K_3=0; In the third step, K_1=K_2=0, K_3=1, and finally, all outputs are optimized simultaneously: so, K_1=K_2=K_3=1.

The optimization design results are shown in Table 3. The design is done with constant motor speed of 2.5 m/s and output thrust of 128±4N. In first design case, only efficiency is optimized. Regarding that there is no limitation on the weight and the power factor, the dimensions of the motor are high and the input frequency is comparatively low; and the power factor takes approximately its minimum value of 0.3057. On the other hand, the primary current density is 3A/mm^2 which leads to high efficiency. The efficiency is 60.17%. In the second case (K_2=1,K_1=K_3=0), only the power factor is optimized. In this case the dimensions of the motor are high as the primary weight is not considered in optimization. The input frequency is 7.6 Hz. The efficiency takes its minimum value; however, a high power factor of 0.9692 is obtained. In the third case (K_1=K_2=0,K_3=1), only the primary weight is optimized. The results show that the dimensions of the motor are reduced to assure minimum weight (3.08Kg), while the primary current density is 6A/mm^2; so, in comparison to case 1, the efficiency is reduced, in this case. In the last case (K_1=K_2=K_3=1), all of the 3 outputs are optimized, simultaneously. In this case, the dimensions of the motor are comparatively low, but higher than their counterparts in case 3. It should be mentioned that in cases 3 and 4 due to low value of the obtained dimensions, the tooth flux density takes its maximum value of 1.6 T. Also, the output thrust in all cases in Table 3 is close enough to desired value and the objective functions are improved considerably in comparison with non-optimized design. For instance the objective function in case 4 of Table 3 is improved from 0.0124 in non-optimized design to 0.0575 in optimal one.

Table 2: design variable constraints

Parameter	Minimum value	Maximum value
Primary current density, A/mm^2	3	6
Primary width, mm	50	250
Secondary sheet thickness, mm	1	5
Slip	0.1	0.5
Air gap length, mm	1	15
Number of pole pairs	2	5
Number of slots/pole/phase	1	4
Slot width to slot pitch ratio	0.4	0.7
Frequency, Hz	1	100
Efficiency, %	30	-
Power factor	0.30	-

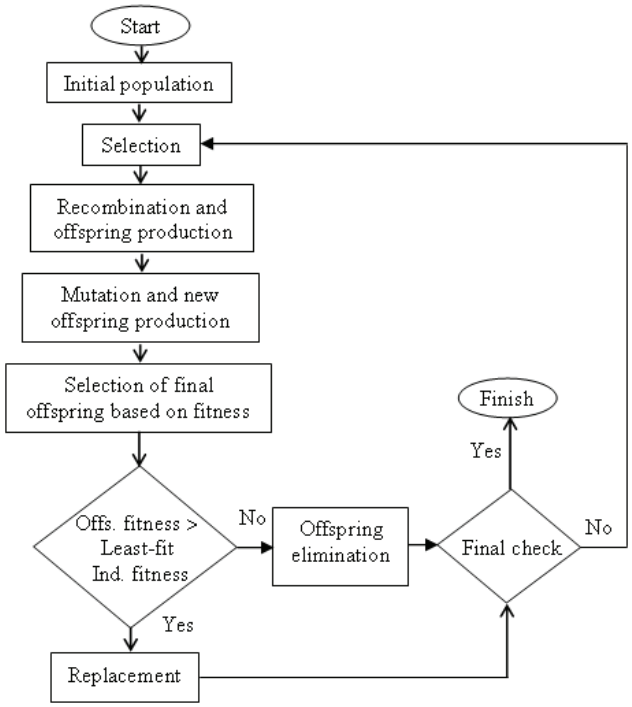

Fig.13. Flowchart for the genetic algorithm

Finite element analysis

In this paper, because of the low speed of the motor, the end effect phenomenon is not considered in the model used for design and optimization. In addition, the permeability of the primary core and secondary back iron was supposed to

be infinity. So, it is necessary to confirm the results of the optimization by finite element method (FEM). To do this, in this section, the optimized design case 4 with limited slots per pole per phase (q) is simulated using 2-D FEM (q is limited to 1). Computer hardware limitations and avoiding the complexity of the model implemented in FEM are the only reasons for limiting q. The specifications of the optimized design example with limited q which is called "case 5" hereafter, are shown in Table 4. In this design, all of the 3 outputs are optimized, simultaneously (K_1=K_2=K_3=1). Fig.14 shows the distribution of the flux density in different parts of the SLIM as it moves in x direction. As the motor moves towards right, the flux wave travels left. It is seen in the figure that the flux density in the primary teeth is around 1T which is near enough to the value obtained by optimization in Table 4. Also, the air-gap and the secondary sheet have the flux density of about 0.44T in most of the areas. Fig.15 illustrates the flux paths in the different parts of the motor. It can be seen that the flux lines are denser in exit end of the motor. It should be mentioned that, the eddy-current and iron core loss are considered in efficiency calculation. The efficiency, power factor and thrust are calculated using FEM. The analytical calculation results are compared with FEM results in Table 5. As seen in this table, the thrust obtained by FEM is slightly lower than that of obtained by analytical calculations. It may partly because of the end effect phenomenon which is not considered in analytical model. However, the results of the two methods are in good agreement with each other. It should be mentioned that, in FEM simulations, in order to confirm the accuracy of the results, the number of meshes were doubled; however, there was no sensible changes in the results. This indicates that the number of selected meshes was enough for the calculations.

Table 3: optimized motor parameter values

Specification	Optimum values (K_1=1, K_2=K_3=0)	Optimum values (K_2=1, K_1=K_3=0)	Optimum values (K_1=K_2=0, K_3=1)	Optimum values (K_1=1, K_2=K_3=1)
Primary current density, A/mm^2	3	3.77	6	6
Primary width, mm	105	240	51.7	50
Sec. sheet thickness, mm	1.2	2.8	1.6	1.3
Air-gap length, mm	1.0	1.0	1.0	1.1
Slip	0.18	0.34	0.49	0.49
No of pole pairs	2	5	2	2
No. of slots/pole/phase	4	4	4	4
Frequency, Hz	16.8	7.6	62.3	44.8
No. of turns/coil, n_{coil}	84	68	84	114
Phase input current, A	2.66	1.66	3.19	2.25
Motor length(L_s), m	0.3615	2.4920	0.1574	0.2188
Tooth width, mm	4.5	12.4	1.0	1.4
Slot width, mm	3	8.4	2.3	3.2
Slot width to slot pitch ratio	0.4	0.4	0.69	0.69
Teeth flux density(B_t), T	0.97	0.103	1.6	1.6
Efficiency, %	60.17	30.00	40.56	39.59
Power factor	0.3057	0.9692	0.3717	0.5399
Primary weight, Kg	19.85	282.97	3.08	3.72
output thrust, N	129.36	127.83	127.12	127.13
Objective function	0.6017	0.9692	0.2345	0.0575

Table 4: optimized SLIM parameters for FEM simulations

Specification	Optimum values (K_1=K_2=K_3=1)
Phase input voltage, V	220
Motor speed, m/s	2.5
Primary current density, A/mm^2	6
Primary width, mm	51.7
Secondary sheet thickness, mm	1.3
Air gap length, mm	1.0
Slip	0.49
Number of pole pairs	2
Number of slots/pole/phase	1
Frequency, Hz	39.0
Number of turns/coil, n_{coil}	451
Phase input current, A	2.33
Motor length(L_s), m	0.2514
Tooth width, mm	9.2
Slot width, mm	12.8
Slot width to slot pitch ratio	0.56
Teeth flux density(B_t), T	1.0
Efficiency, %	38.57
Power factor	0.5382
Primary weight, Kg	4.86
Output thrust, N	127.85
Objective function	0.0427

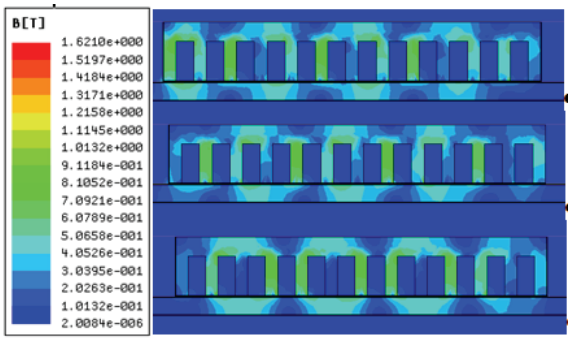

Fig.14. Flux density distribution in different parts of the SLIM

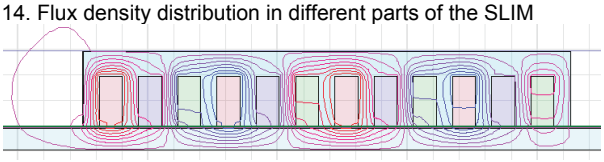

Fig.15. Flux paths in the SLIM

Table 5: The calculation and FEM results

Parameter	Analytical model	FEM
Efficiency, %	38.57	36.2
Power factor	0.5382	0.508
Primary weight, Kg	4.86	-
Thrust, N	127.85	121.2
Objective function	0.0427	-

Conclusion

A simple and applicable procedure based on equivalent circuit model is proposed to design the SLIM. The effect of the different design variables on the performance of the machine is investigated. A multi-objective optimization method based on the genetic algorithm is employed to optimize the SLIM design. 9 effective variables are chosen for design optimizations. The analytical optimization results show noticeable improvements in the objective functions. 2D finite element method is employed to confirm the precision of the equivalent circuit model and the effectiveness of the optimization method. The FEM results which considers the end effects are in good agreement with

the analytical results. This confirms the validity of the proposed optimal design in low speeds.

REFRENCES

[1] Mirsalim M., Doroudi A., Moghani J. S., Obtaining the operating characteristics of linear induction motors: a new approach, *IEEE Trans. Magn*, 38(2002), No. 2, 1365-1370.

[2] Creppe R. C.,. Ulson J. A. C, Rodrigues J. F., Influence of design parameters on linear induction motor end effect, *IEEE Trans. Energy Convs*, 23(2008), No. 2, 358-362.

[3] Nonaka S., Investigation of equivalent circuit quantities and equations for calculation of characteristics of single-sided linear induction motors (LIM), *Electrical Engineering in Japan*, 117(1996), No. 2, 107-121.

[4] Nonaka S., Investigation of equations for calculation of secondary resistance and secondary leakage reactance of single-sided linear induction motors, *Electrical Engineering in Japan,* 122(1998), No. 1, 60-67.

[5] Laithwaite E. R., Nasar S. A., Linear-Motion Electrical Machines, *Proc. of IEEE*, 58(1970), No.4, 531-542.

[6] Yoon S., Hur J., Hyun D., A method of optimal design of single-sided linear induction motor for transit, *IEEE Trans. Magn*, 33(1997), No. 5, 4215-4217.

[7] Osawa S., Wada M., Karita M., Ebihara D., T. Yokoi, Light-weight type linear induction motor and its characteristics, *IEEE Trans. Magn*, 28(1992), No. 4, 3003-3005.

[8] Kitamura M., Hino N., Nihei H., M. Ito, a direct search shape optimization based on complex expressions of 2-dimentional magnetic fields and forces, *IEEE Trans. Magn*, 34(1998), No. 5, 2845-2848.

[9] Laporte B., Takorabet N., Vinsard G., An approach to optimize winding design in linear induction motors, *IEEE Trans. Magn*, 33(1997), No. 2, 1844-1847.

[10] Mishima T., Hiraoka M., Nomura T., A study of the optimum stator winding arrangement of LIM in maglev systems, *IEEE Inter. Conf. on Electric Machines Drives*, *IEMDC*, (2005), 1238-1242.

[11] Hassanpour Isfahani A., Lesani H., Ebrahimi B. M., Design Optimization of Linear Induction Motor for Improved Efficiency and Power Factor, *IEEE Inter. Conf. on Electric Machines Drives, IEMDC*, (2007), 988-991.

[12] Hassanpour Isfahani A., Ebrahimi B. M., Lesani H., Design Optimization of a Low-Speed Single-Sided Linear Induction Motor for Improved Efficiency and Power Factor, *IEEE Trans. Magn.*, 44(2008), No. 2, 266-272.

[13] Lucas C., Nasiri G. Z., Tootoonchian F., Application of an imperialist competitive algorithm to design of linear induction motor, *Elsv. Engy. Conv. & Mang*, 51(2010), 1407-1411.

[14] Gieras J. F., *Linear induction drives*, *Oxford University Press, Inc., New York*, (1994).

[15] Boldea I., Nasar S. A., *linear motion electromagnetic devices*, *Taylor & Francis*, New York (2001).

[16] Nasar S. A., Boldea I., *linear electric motors*, *Prentice-Hall, Inc., Englewood Cliffs*, New Jersey, (1987).

[17] Laithwaite E. R., *Induction machines for special purposes*, *George Newnes Limited*, London (1996).

[18] Sumathi S., Surekha P., Computational intelligence paradigms: theory and applications using MATLAB, *CRC Press, Taylor & Francis*, New York (2010).

***Authors**: Abbas Shiri, Iran University of science & Technology, Narmak, Tehran, Iran, E-mail: abbas_shiri@iust.ac.ir; prof. Abbas Shoulaie, Iran University of science & Technology, Narmak, Tehran, Iran, E-mail:shoulaie@iust.ac.ir*